Force Field Parametrization for Gadolinium Complexes Based on ab Initio Potential Energy Surface Calculations

Alessandra Villa,* Ugo Cosentino, and Demetrio Pitea

Dipartimento di Scienze dell'Ambiente e del Territorio, Università degli Studi di Milano-Bicocca, P.zza della Scienza 1, 20126 Milano, Italy

Giorgio Moro

Dipartimento di Biotecnologie e Bioscienze, Università degli Studi di Milano-Bicocca, P.zza della Scienza 2, 20126 Milano, Italy

Alessandro Maiocchi

Bracco SpA, Via E. Folli 50, 20134 Milano, Italy

Received: January 10, 2000

The recent design of new magnetic resonance imaging (MRI) contrast agents is oriented toward the synthesis of gadolinium(III) complexes with ligands presenting formally neutral (amidic or alcoholic) or anionic (phosphinic) oxygen donor atoms. This paper presents the molecular mechanics (MM) parametrization of Gd interactions with amidic, alcoholic and phosphinic oxygen donor atoms, with the aim of supporting experimental effort. The parametrization is performed on the basis of a previously developed procedure applied to the parametrization of Gd interactions with polyamino carboxylate (PAC) ligands. Within the framework of valence force fields, the parameters for Gd−ligand interactions are determined by fitting the empirical potential to the ab initio potential energy surface (PES) of $[Gd\cdot\mathbf{3}\cdot OH_2]^{3+}$, $[Gd\cdot\mathbf{5b}\cdot OH_2]^{3+}$, and $[Gd\cdot\mathbf{8a}]^{1-}$. Ab initio calculations were performed at the restricted Hartree−Fock (RHF) level by using an effective core potential (ECP) that includes 4f electrons in the core, an optimized valence basis set for the metal, and the 3-21G basis set for the ligand. Sampling of the PES is performed by moving the ion into the frozen coordination cage of the ab initio optimized geometries. The energy and first derivatives, with respect to the Cartesian coordinates of the metal and donor atoms, were calculated for each generated structure. Two sets of parameters, with the electrostatic contribution turned on or off in the force fields, were determined. To test the quality of the derived parameters and their transferability to other Gd complexes, MM calculations were performed on several gadolinium complexes. The results show that both sets of parameters provide reliable molecular geometries, but it is necessary to include the electrostatic contribution in the force fields to correctly reproduce the conformational energies.

I. Introduction

Over the past 10 years there has been renewed interest in the complexation chemistry of lanthanides. One aspect, in particular, centers on the in vivo application of paramagnetic gadolinium complexes as contrast agents in magnetic resonance imaging (MRI), which, over the last two decades, has become an important tool in modern medical diagnostics.[1] Complexes of the highly paramagnetic Gd(III) ion with polyamino carboxylate (PAC) ligands are the most widely employed contrast agents for MRI[1a] and complexes with DOTA[2] (**1**) and DTPA (**2**) (Figure 1) are currently used in clinical practice.

The experimental investigation of the behavior of Gd complexes in solution is not easily performed as the usual techniques, such as NMR spectroscopy, are not suitable due to the high magnetic moment of the Gd ion. Thus, a theoretical approach to these complexes could provide a valid tool for the characterization of their molecular properties.

* To whom correspondence should be addressed: Dr. Alessandra Villa, Dipartimento di Chimica Fisica ed Elettrochimica Università degli Studi di Milano, Via Golgi 19, 20133 Milano, Italy. Phone, ++39 02 26603247; fax, ++39 02 70638129; e-mail: a.villa@csrsrc.mi.cnr.it.

Given the molecular dimensions of such systems, advantage can be taken of the effective core potential (ECP) approximation through ab initio calculations. By restricting quantomechanical treatment to the valence shell of the lanthanides, and incorporating the main relativistic effects into self-consistent field (SCF) calculations,[3,4] ECP reduces the computational effort but still provides reliable results. Alternatively, molecular mechanics (MM) provides a very cheap and accurate computational approach to study the conformational behavior of coordination compounds when the metal−ligand interactions are accurately parametrized in the force fields.

In a previous paper[5] reliable computational methods for modeling Gd−PAC complexes were set up: the accuracy of ab initio methods, using ECP approximation for the ion, was tested and a properly parametrized force field within the MM method was developed for the interactions of Gd with amminic nitrogens and carboxylic oxygen donor atoms.

In the case of lanthanides, force fields derived from experimental data were available.[6] However, a more general strategy based on ab initio calculations for the parametrization of metal−

10.1021/jp000121l CCC: $19.00
Published on Web 03/29/2000

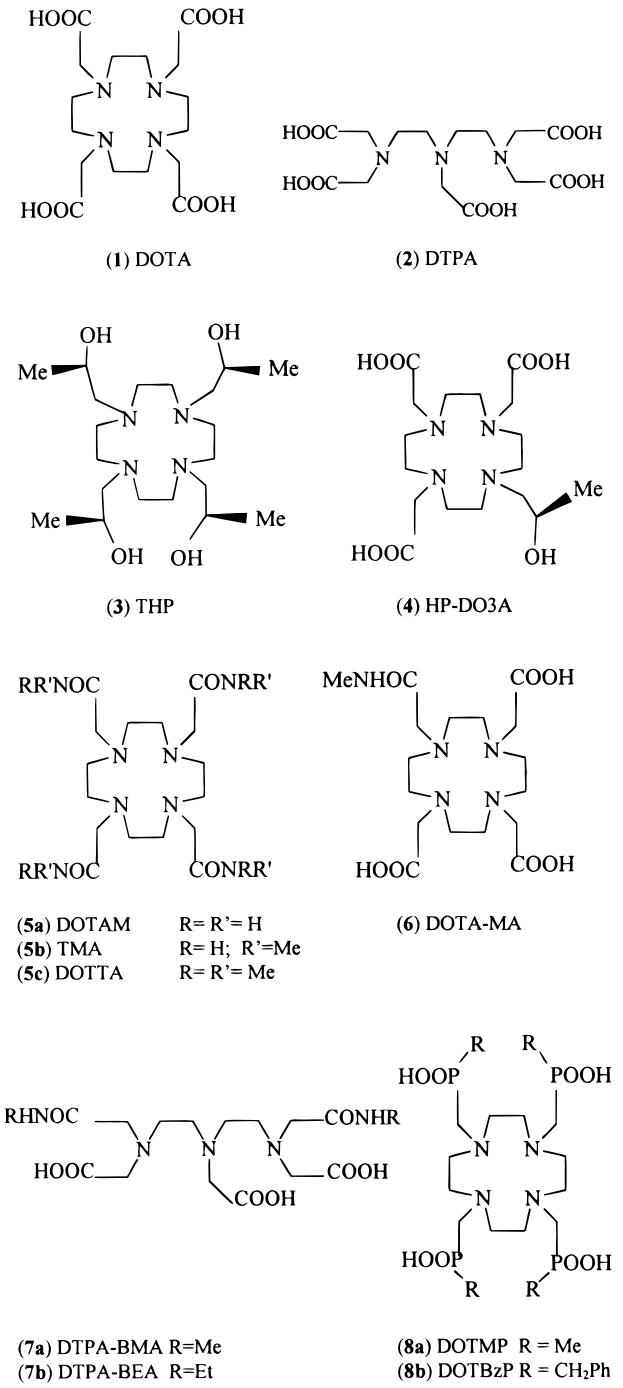

Figure 1. Molecular structures and numbering of the considered ligands.

ligand interactions was preferred, because experimental data on lanthanide complexes are available only for a few ligand classes.

The strategy adopted for the extension of a predefined "organic" force fields to metal complexes relies on the derivation of metal−ligand parameters from ab initio results and on the use of already available parameters for the organic part of the complex. Although the quality of the force field parameters in this procedure depends on the theory level of the quantum mechanical calculations, it is in no way limited by a lack of experimental data.

Note that for this procedure, due to the redistribution of electron density upon coordination, there is generally a need to refine the parameters for intraligand interactions.[7,8]

The Gd−PAC ligand parameters were obtained[5] by fitting the MM empirical potential to the ab initio potential energy surface (PES), using a procedure[9] that involves the fitting of ab initio energies and energy derivatives.

The design of new MRI contrast agents is today oriented toward gadolinium complexes with ligands presenting formally neutral (amidic or alcoholic) or anionic (phosphinic) oxygen donor atoms and this has prompted us to investigate the parametrization of MM force fields for complexes of gadolinium with ligands presenting amidic, alcoholic, and phosphinic oxygen donor atoms, our aim being to find theoretical support for the design and synthesis of new Gd(III) complexes. The extension of the force fields to new classes of complexes leads to two main goals: the validation of the previously developed parametrization procedure and the confirmation of the transferability of the derived parameters to a larger set of compounds.

The investigation concerns structural and energetic aspects of Gd complexes with octadentate ligands presenting alcoholic (**3**, THP; **4**, HP-DO3A), amidic (**5a**, DOTAM; **5b**, TMA; **5c**, DOTTA; **6**, DOTA-MA; **7a**, DTPA-BMA), and phosphinic groups (**8a**, DOTMP). The molecular structures and the identification numbers of the considered ligands are reported in Figure 1 (Note 2 gives the abbreviated ligand names); Figure 2 shows the coordination mode to the ion of the considered classes of ligands.

The experimental evidence reveals that in these complexes, both in the solid state[10−14] and in solution,[15] the ion is enneacoordinate, with the ninth coordination site occupied by one water molecule. The only exception is the complexes with phosphinic ligands (i.e., **8a** and **8b)**, that present octacoordination due to the steric hindrance of the phosphinic groups that preclude water molecule coordination.[15,16]

It should be noted that the presence of one (or more) water molecules coordinated to the ion is particularly relevant to the use of these complexes as MRI contrast agents. In fact, the ability of the complex to enhance image contrast is related to its relaxivity, i.e., its efficiency in increasing the water protons relaxation rate via dipolar interaction. Also chemical exchange between the ion-coordinated water molecule and the bulk solvent affects the relaxivity. For this reason, all the systems, apart from $[Gd\cdot\mathbf{8a}]^{1-}$, were investigated explicitly considering the ion-coordinated water molecules. Because of the diagnostic applications of such systems, the species stable at around pH 7 were paid particular attention. Available pK_a experimental values for amidic NH deprotonation in $[Gd\cdot\mathbf{5b}\cdot OH_2]^{3+}$ (pK_{a1} = 11.02; pK_{a2} = 11.89)[15] and for alcoholic OH deprotonation in $[Gd\cdot\mathbf{4}\cdot OH_2]$ (pK_a = 11.36)[17] show that at neutral pH, deprotonation of the amidic and of the alcoholic protons does not occur. Consequently, the investigation of complexes **3**−**7** involved the amidic NH and the alcoholic OH species, as sketched in Figure 2.

II. Methods and Results

Ab initio Calculations. Ab initio calculations were performed at the RHF level with the Gaussian94 program[18] using the 46 + 4f ^{n} core electrons (1s−4d, 4f^n) ECP,[19] and the [5s4p3d]-GTO valence basis set for the metal.[19] As previously shown,[5,20] the inclusion of 4f electrons in the core makes this ECP appropriate for molecular systems of large dimensions. For the ligand atoms the 3-21G basis set was used: the results obtained on Gd−PAC complexes show[5] that the computational effort that was needed to use better ligand basis sets was not counterbalanced by a significant improvement in the calculated geometries.

Full geometry optimizations of compounds $[Gd\cdot\mathbf{3}\cdot OH_2]^{3+}$, $[Gd\cdot\mathbf{5b}\cdot OH_2]^{3+}$, and $[Gd\cdot\mathbf{8a}]^{1-}$ were performed starting from

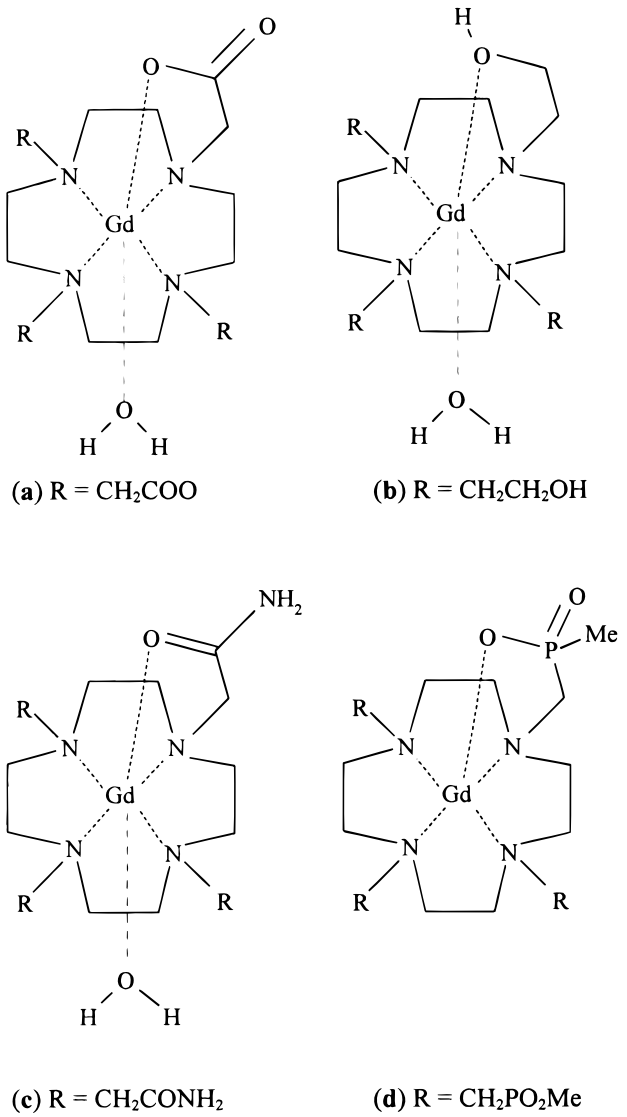

Figure 2. Coordination mode to the ion of ligands presenting: (a) carboxylic; (b) alcoholic; (c) amidic; (d) phosphinic oxygen donor atoms.

the crystallographic structures[10,12,16] of $[Eu\cdot\mathbf{3}\cdot OH_2]^{3+}$, $[Gd\cdot\mathbf{5b}\cdot OH_2]^{3+}$, and $[Y\cdot\mathbf{8b}]^{1-}$.

The experimental and calculated values of the main geometrical parameters of the complexes are reported in Table 1, while Table 2 shows the root means square (rms) values of the experimental and ab initio structures, calculated on the Cartesian coordinates. For comparison, the results[5] on the PAC complexes $[Gd\cdot\mathbf{1}\cdot OH_2]^{1-}$ and $[Gd\cdot\mathbf{2}\cdot OH_2]^{2-}$ are also reported.

Force Field Parametrization and MM Calculations. *Adopted Force Fields.* The MM calculations were carried out by the Sybyl 6.3 molecular software package[21] using TRIPOS force fields[22] that are purely harmonic and without cross-terms. Valence interactions involving Gd are handled within the framework of the point on a sphere (POS) approach.[23] In the POS scheme, the Gd−L stretching interactions (L denotes ligand atoms coordinated to the metal) are included in the force fields, while the L−Gd−L bending terms are replaced by nonbonding interactions between the donor atoms (L···L); moreover, no account is taken of either torsional interactions involving Gd−L bonds or van der Waals interactions involving the metal. The calculations were performed with and without the electrostatic contribution to the force fields: when included, a distance-dependent dielectric constant was used. The atomic charges were obtained by fitting the RHF/6-31G* molecular electrostatic potential (MEP)[24] of the complexes by the Merz−Kollman method.[25]

Metal Independent Parameters. As in other applications of MM to coordination compounds,[7,8] the TRIPOS force fields parameters used to model the interactions in the free ligand were assumed to be transferable to the ligand portion of the complex. However, due to electron density redistribution upon coordination, a refinement of the parameters for some intraligand interactions was required: the values of the C.3−C.3, C.2−C.3, and P.3−C.3 stretching and the O.3−C.2−O.2, O.p−P.3−O.2, and O.am−C.2−N.am bending parameters (note 26 lists the adopted atom types) were determined by trial and error to fit the ab initio calculated structures (Table 3).

Metal-Dependent Parameters. The previously developed parameters[5] for stretching and bending interactions involving Gd and aminic nitrogens (N.4), carboxylic oxygens (O.3), and water oxygens (O.w) were used.

The new parameters describing the stretching (Gd−O.h, Gd−O.am, and Gd−O.p) and the bending (Gd−O.h−C.3, Gd−O.h−H, Gd−O.am-C.2, and Gd−O.p−P.3) interactions were determined by fitting the empirical potential to the ab initio PES of compounds $[Gd\cdot\mathbf{3}\cdot OH_2]^{3+}$, $[Gd\cdot\mathbf{5b}\cdot OH_2]^{3+}$, and $[Gd\cdot\mathbf{8a}]^{1-}$, as described later. For the L−Gd−L−X torsions (X denotes ligand atoms not coordinated to the metal), the torsional constant values were set to zero; for the Gd−L−X−X torsions, TRIPOS generalized parameters were used. van der Waals interactions involving the Gd ion were omitted. For the 1,3 nonbonding interactions standard van der Waals TRIPOS parameters were used for the L donor atoms, and when the electrostatic contribution was turned on the electrostatic interactions between the L atoms were considered.

For the stretching and bending interactions the previously developed parametrization strategy[5] was followed. Sampling of the ab initio PES was performed by moving the Gd ion inside the frozen coordination cage of the complex. This allowed the mapping of energy changes associated with modifications of the internal coordinates involving the ion. In fact, the aim of parametrization is to determine the metal−ligand parameters, while the intraligand interactions are described by the predefined force fields.

Depending on the metal−ligand interaction to be parametrized, an appropriate target compound was chosen: $[Gd\cdot\mathbf{3}\cdot OH_2]^{3+}$ was used to parametrize the Gd-alcoholic oxygen interactions, $[Gd\cdot\mathbf{5b}\cdot OH_2]^{3+}$ the Gd-amidic oxygen interactions, and $[Gd\cdot\mathbf{8a}]^{1-}$ the Gd-phosphinic oxygen interactions.

The sampling of the PES of each compound was performed by generating new conformations, with relative energies of up to 20 kcal mol^{1-} above the minimum, starting from the RHF/3-21G optimized geometries. The generated distorted structures were checked to verify that the internal coordinates involving the metal were well sampled around the equilibrium values; on average, a range of 0.4 Å for Gd−L bond distances and 10° for Gd−L−X angles was obtained.

For each sampled structure, the energy and the first derivatives with respect to the atomic Cartesian coordinates were calculated at the RHF/3-21G level. The first derivatives with respect to the Cartesian coordinates of the Gd atom and the oxygen donor atoms involved in the interactions to be parametrized were included in the fitting of the empirical potential. Second energy derivatives were not considered due to the intrinsic limitations imposed by harmonic-diagonal force fields, like TRIPOS, on fitting information contained in the ab initio Hessian matrix.

TABLE 1: Values of the Main Geometrical Parameters of Experimental and Calculated (ab Initio and MM) Structures of Gd Complexes with Ligands 1−8[a]

	exp	RHF/3-21G	MM Set 1	MM Set 1′ [b]
[Gd·**1**·OH_2]$^{1-}$				
ref	5	5	5	5
Gd−N	2.655 (0.006)	2.751 (0.021)	2.756 (0.019)	2.713 (0.001)
Gd−O.3	2.365 (0.004)	2.334 (0.035)	2.357 (0.017)	2.339 (0.001)
Gd−O.w	2.456	2.515	2.495	2.451
Gd−Pn[c]	1.633	1.744	1.702	1.594
Gd−Po[d]	0.719	0.625	0.512	0.705
ϕ[e]	36.0 (5.8)	39.0 (1.4)	41.7 (1.4)	38.7 (0.1)
[Gd·**2**·OH_2]$^{1-}$				
ref	5	5	5	5
Gd−N	2.389 (0.019)	2.369 (0.057)	2.372 (0.016)	2.346 (0.009)
Gd−O.3	2.666 (0.056)	2.788 (0.060)	2.747 (0.036)	2.737 (0.017)
Gd−O.w	2.463	2.614	2.517	2.452
[Gd·**3**·OH_2]$^{3+}$				
ref	10[f]			
Gd−N	2.683 (0.024)	2.654 (0.014)	2.797 (0.026)	2.714 (0.000)
Gd−O.h	2.411 (0.024)	2.447 (0.007)	2.526 (0.003)	2.580 (0.020)
Gd−O.w	2.512	2.725	2.481	2.589
Gd−Pn[c]	1.680	1.603	1.739	1.603
Gd−Po[d]	0.894	0.990	1.041	1.008
ϕ[e]	−19.8 (0.8)	−19.4 (1.3)	−15.3 (9.1)	−22.6 (0.6)
[Gd·**4**·OH_2]				
ref	11			
Gd−N	2.648 (0.007)		2.699 (0.020)	2.716 (0.027)
Gd−O.3	2.348 (0.038)		2.332 (0.007)	2.336 (0.006)
Gd−O.w	2.507		2.469	2.45
Gd−O.h	2.397		2.475	2.529
Gd−Pn[c]	1.610		1.598	1.597
Gd−Po[d]	0.746		0.724	0.734
ϕ[e]	37.9 (0.7)		40.7 (0.6)	37.9 (1.1)
[Gd·**5b**·OH_2]$^{3+}$				
ref	12			
Gd−N	2.636 (0.014)	2.711 (0.000)	2.740 (0.003)	2.726 (0.001)
Gd−O.am	2.388 (0.049)	2.388 (0.007)	2.371 (0.013)	2.383 (0.002)
Gd−O.w	2.461	2.412	2.509	2.470
Gd−Pn[c]	1.590	1.642	1.617	1.570
Gd−Po[d]	0.741	0.687	0.506	0.773
ϕ[e]	38.3 (1.3)	37.6 (1.3)	43.6 (0.6)	39.2 (0.3)
[Gd·**6**·OH_2]				
ref	13			
Gd−N	2.675 (0.049)		2.733 (0.009)	2.708 (0.007)
Gd−O.3	2.358 (0.021)		2.347 (0.010)	2.339 (0.002)
Gd−O.am	2.392		2.355	2.368
Gd−O.w	2.428		2.475	2.453
Gd−Pn[c]	1.649		1.644	1.578
Gd−Po[d]	0.685		0.605	0.731
ϕ[e]	38.8 (0.9)		41.6 (1.1)	38.8 (0.8)
[Gd·**7a**·OH_2]				
ref	14[g]			
Gd−N	2.697 (0.060)		2.701 (0.035)	2.723 (0.019)
Gd−O.3	2.365 (0.018)		2.334 (0.011)	2.343 (0.009)
Gd−O.am	2.394 (0.061)		2.363 (0.008)	2.388 (0.013)
Gd−O.w	2.425		2.532	2.449
[Gd·**8a**]$^{1-}$				
ref	16[h]			
Gd−N	2.662 (0.015)	2.758 (0.000)	2.735 (0.000)	2.720 (0.000)
Gd−O.p	2.255 (0.047)	2.283 (0.000)	2.218 (0.000)	2.241 (0.000)
Gd−Pn[c]	1.639	1.754	1.644	1.609
Gd−Po[d]	0.972	0.907	0.871	1.101
ϕ[e]	−29.0 (1.1)	−32.5 (0.0)	−34.1 (0.0)	−28.6 (0.0)

[a] The average values are reported with standard deviations in parentheses. Distances (Å), angles (deg). [b] The primed symbol is used when the electrostatic contribution is turned off. [c] Distance of Gd from the least-squares plane defined by the N atoms, Pn. [d] Distance of Gd from the least-squares plane defined by the O atoms, Po. [e] Staggering of the P_O and P_N planes. [f] Experimental data refers to [Eu·**3**·OH_2]$^{3+}$. [g] Experimental data refers to [Gd·**7b**·OH_2]. [h] Experimental data refers to [Y·**8b**·]$^{1-}$.

Parametrization was performed by minimizing the object function **S**, defined as the weighted sum of the squared deviations between ab initio and MM quantities:

$$\mathbf{S} = w_E \sum_{k=1}^{N-1} [\Delta E_k^{\circ} - \Delta E_k(\mathbf{p})]^2 + w_g \sum_{k=1}^{N} \sum_{i=1}^{M} \sum_{j=1}^{3} \left[\frac{\partial E_k^{\circ}}{\partial x_{i,j}} - \frac{\partial E_k(\mathbf{p})}{\partial x_{i,j}} \right]^2$$

where N is the number of sampled conformations and M the number of atoms whose derivatives are considered; ΔE_k° and $\Delta E_k(\mathbf{p})$ are, respectively, the ab initio and the MM relative energies of the kth structure; $(\partial E_k^{\circ}/\partial x_{i,j})$ and $(\partial E_k(\mathbf{p})/\partial x_{i,j})$ are respectively the ab initio and the MM first derivatives with respect to the jth Cartesian coordinates of the ith atom in the kth structure. The values for the w_E and w_g scaling factors were assigned to ensure that energy and first derivative squared deviations contribute in a balanced way to the object function.[27] The empirical potential parameters (**p** vector) were calculated,

TABLE 2: Rms Values (Å) between the Experimental, ab Initio, and MM (Set 1 and Set 1′)[a] Structures of Gd Complexes with Ligands 1−8[b]

	I			II		
	RHF 3-21G	Set 1	Set 1′	RHF 3-21G	Set 1	Set 1′
RHF/3-21G						
[Gd·**1**·OH_2]$^{1-}$ [c]		0.132	0.186		0.161	0.182
[Gd·**3**·OH_2]$^{3+}$		0.248	0.123		0.180	0.112
[Gd·**5b**·OH_2]$^{3+}$		0.186	0.072		0.191	0.165
[Gd·**8a**]$^{1-}$		0.089	0.144		0.255	0.181
Average		0.164	0.131		0.197	0.160
Exp						
[Gd·**1**·OH_2]$^{1-}$ [c]	0.058	0.152	0.094	0.285	0.179	0.212
[Gd·**3**·OH_2]$^{3+}$ [d]	0.068	0.248	0.117	0.140	0.210	0.195
[Gd·**5b**·OH_2]$^{3+}$	0.103	0.184	0.082	0.167	0.181	0.148
[Gd·**8a**]$^{1-}$ [e]	0.094	0.124	0.108	0.215	0.168	0.145
[Gd·**4**·OH_2]		0.091	0.102		0.210	0.197
[Gd·**6**·OH_2]		0.126	0.099		0.190	0.185
[Gd·**7a**·OH_2][f]		0.335	0.173		0.390	0.283
[Gd·**2**·OH_2]$^{1-}$ [c]		0.217	0.175		0.314	0.276
Average	0.081	0.185	0.119	0.202	0.230	0.205

[a] The primed symbol is used when the electrostatic contributions is turned off. [b] Rms are calculated on the cartesian coordinates of (I) the atoms of the coordination cages (Gd and the ligand coordinated atoms); (II) all atoms, but hydrogens. Average rms values are also reported. [c] Values from ref 5. [d] Experimental data[10] refer to [Eu·**3**·OH_2]$^{3+}$. [e] Experimental data[16] refer to [Y·**8b**]$^{1-}$. [f] Experimental data[14] refer to [Gd·**7b**·OH_2].

TABLE 3: Default and Modified Force Field Parameters[a] for the Intraligand Interactions Determined by Trial and Error Procedure

metal-independent parameters	default	modified
$r^0_{C.3-C.3}$	1.540	1.510[b]
$K_{C.3-C.3}$	633.6	650.0[b]
$r^0_{C.3-C.2}$	1.501	1.530[b]
$K_{C.3-C.2}$	639.0	639.0[b]
$r^0_{P.3-C.3}$	1.83	1.87
$K_{P.3-C.3}$	407.6	407.6
$\vartheta^0_{O.3-C.2-O.2}$	120.0	126.0[b]
$K_{O.3-C.2-O.2}$	0.030	0.030[b]
$\vartheta^0_{O.p-P.3-O.2}$	109.5	114.0
$K_{O.p-P.3-O.2}$	0.020	0.020
$\vartheta^0_{O.am-C.2-N.am}$	120.0	124.0
$K_{O.am-C.2-N.am}$	0.024	0.024

[a] r^0 (Å); ϑ^0 (deg); K_r (kcal mol^{1-} Å^{2-}); K_ϑ (kcal mol^{1-} deg^{2-}); K_τ (kcal mol^{1-}). [b] Previously[5] determined values.

using a purposely developed computer code, by a least-squares procedure.

The parametrization procedure was performed both including and omitting the electrostatic contribution to the force fields. This resulted in two sets of force field parameters (Table 4), labeled as Set 1 and Set 1′ respectively with and without the electrostatic contribution included.

The quality of the fitting of the empirical potential to the RHF/3-21G PES of the three quoted complexes is reported in Table 5 for both sets.

To test the quality of the derived parameters, MM calculations were performed on the complexes of Gd with ligands **3**, **5b**, and **8a**, all involved in the parametrization (training set); moreover, to test parameter transferability, also the Gd complexes with ligands **4**, **6**, and **7a** were investigated (test set).

Table 1 shows the MM calculated values for the main geometrical parameters, Table 2 the rms values between the MM optimized structures and the experimental and ab initio ones calculated on the Cartesian coordinates.

TABLE 4: Force Field Parameters[a] for the Gd−ligand Interactions Determined by Fitting of the RHF/3-21G (Set 1 and Set 1′)[b] PES of Compounds [Gd·1·OH_2]$^{1-}$,[5] [Gd·3·OH_2]$^{3+}$, [Gd·5b·OH_2]$^{3+}$, and [Gd·8a]$^{1-}$

metal−dependent param	Set 1	Set 1′
electrostatic contribution	yes	no
$r^0_{Gd-N.4}$	2.601	2.734
$K_{Gd-N.4}$	75.0	75.4
$r^0_{Gd-O.3}$	2.287	2.344
$K_{Gd-O.3}$	147.2	149.4
$r^0_{Gd-O.w}$	2.497	2.445
$K_{Gd-O.w}$	125.5	130.6
$r^0_{Gd-O.am}$	2.300	2.374
$K_{Gd-O.am}$	140.8	146.5
$r^0_{Gd-O.h}$	2.440	2.512
$K_{Gd-O.h}$	131.8	140.6
$r^0_{Gd-O.p}$	2.230	2.25
$K_{Gd-O.p}$	175.3	179.9
$\vartheta^0_{Gd-N.4-C.3}$	108.2	111.3
$K_{Gd-N.4-C.3}$	0.027	0.027
$\vartheta^0_{Gd-O.3-C.2}$	127.8	128.8
$K_{Gd-O.3-C.2}$	0.045	0.046
$\vartheta^0_{Gd-O.w-H.w}$	119.5	118.5
$K_{Gd-O.w-H.w}$	0.012	0.012
$\vartheta^0_{Gd-O.am-C.2}$	117.8	123.5
$K_{Gd-O.am-C.2}$	0.045	0.046
$\vartheta^0_{Gd-O.h-C.3}$	116.1	124.4
$K_{Gd-O.h-C.3}$	0.045	0.045
$\vartheta^0_{Gd-O.h-H}$	125.4	131.8
$K_{Gd-O.h-H}$	0.012	0.013
$\vartheta^0_{Gd-O.p-P.3}$	130.5	127.9
$K_{Gd-O.p-P.3}$	0.046	0.048
$K_{*-O.h-C.3-*}$[c]	1.2 (+3)	
$K_{*-O.am-C.2-*}$[c]	4.50 (−2)	
$K_{*-O.p-P.3-*}$[c]	0.4 (+3)	

[a] r^0 (Å); ϑ^0 (deg); K_r (kcal mol^{1-} Å^{2-}); K_ϑ (kcal mol^{1-} deg^{2-}); K_τ (kcal mol^{1-}). [b] The primed symbol means the omission of electrostatic contribution in the force field. [c] Torsional force constant K_τ and torsional periodicity (in parentheses).

III. Discussion

Ab Initio Calculations. The RHF/3-21G optimized geometries of compounds [Gd·**3**·OH_2]$^{3+}$, [Gd·**5b**·OH_2]$^{3+}$, and [Gd·**8a**]$^{1-}$ present a distorted square antiprism coordination polyhedron, capped by one water molecule in the complexes with **3** and **5b**. The nitrogen atoms form a square pyramid with the gadolinium ion forming the apex; the four oxygen donor atoms are involved in a similar, but flattened, square pyramid. The tetraaza macrocyclic ring adopts a [3333] square conformation. These results agree with the crystallographic data[10,12,16] on [Eu·**3**·OH_2]$^{3+}$, [Gd·**5b**·OH_2]$^{3+}$, and [Y·**8b**]$^{1-}$.

It is well-known from experimental evidence that DOTA and DOTA-like complexes both in the solid state and in solution can present two conformational isomers. In fact, the pendent arms can be oriented around the ion in a propeller-like manner, assuming a clockwise or a counterclockwise orientation. In the two isomers the parallel squares, defined by the nitrogen and the oxygen atoms, are staggered by a ϕ angle (Figure 3) of opposite sign. Depending on the ϕ value the isomers are labeled antiprismatic (**A**, $\phi > 0°$) or inverted antiprismatic (**IA**, $\phi < 0°$).

In the case of [Gd·**3**·OH_2]$^{3+}$, both the **A** and the **IA** isomers are present in the crystallographic cell of the europium complex.[10] Ab initio calculations were performed only on the **IA** isomer as its crystallographic structure was the best resolved; the results prove this isomer to be a stationary point on the PES.

In the case of the complex of Gd with **5b** only the **A** isomer is present in the solid state, while for the yttrium complex with

TABLE 5: Fitting of the Empirical Potential (Set 1 and Set 1′)[a] to the RHF/3-21G PES of Compounds $[Gd\cdot1\cdot OH_2]^{1-}$, $[Gd\cdot3\cdot OH_2]^{3+}$, $[Gd\cdot5b\cdot OH_2]^{3+}$, and $[Gd\cdot8a]^{1-}$; RMS,[b] RRMS,[c] and Maximum Deviations between ab initio and MM Relative Energies (ΔE) and Gadolinium Gradient Norm ($||g_{Gd}||$)[d]

	N	ΔE			$\|\|g_{Gd}\|\|$		
		RMS kcal mol^{1-}	RRMS (%)	max dev kcal mol^{1-}	RMS kcal mol^{1-} Å^{1-}	RRMS %	max dev kcal mol^{1-} Å^{1-}
$[Gd\cdot\mathbf{1}\cdot OH_2]^{1-}$ [e]	7						
Set 1		0.78	8.7	1.82	11.1	14.7	17.6
Set 1′		0.57	6.3	0.96	9.9	12.8	19.2
$[Gd\cdot\mathbf{3}\cdot OH_2]^{3+}$	7						
Set 1		0.97	13.5	1.78	11.1	17.5	23.7
Set 1′		0.90	12.5	1.65	11.7	18.5	21.0
$[Gd\cdot\mathbf{5b}\cdot OH_2]^{3+}$	12						
Set 1		0.29	4.2	0.55	13.6	21.1	23.0
Set 1′		0.52	7.6	0.77	4.9	7.7	8.5
$[Gd\cdot\mathbf{8a}]^{1-}$	12						
Set 1		0.67	8.7	2.07	9.1	11.8	24.3
Set 1′		0.72	9.6	1.98	9.1	11.8	27.0

[a] The primed symbol is used when the electrostatic contributions is turned off. [b] RMS $= [\Sigma_k(X_k^\circ - X_k(\mathbf{p}))^2/N]^{1/2}$: N are the sampled conformations, X° and $X(\mathbf{p})$ are the ab initio and MM calculated quantities. [c] RRMS $= [\Sigma_k(X_k^\circ - X_k(\mathbf{p}))^2/\Sigma_k(X_k^\circ)^2]^{1/2} \times 100$. [d] The number of the sampled conformations for each complex (N) is also reported. [e] Values from ref 5.

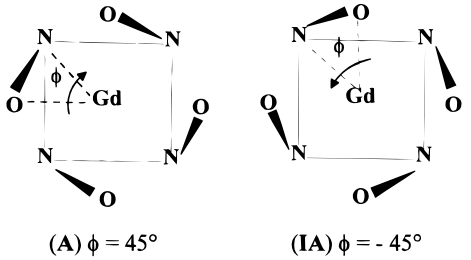

Figure 3. Staggering (ϕ angle) between the nitrogen and oxygen planes in an ideal antiprismatic (**A**) and inverted antiprismatic (**IA**) arrangement.

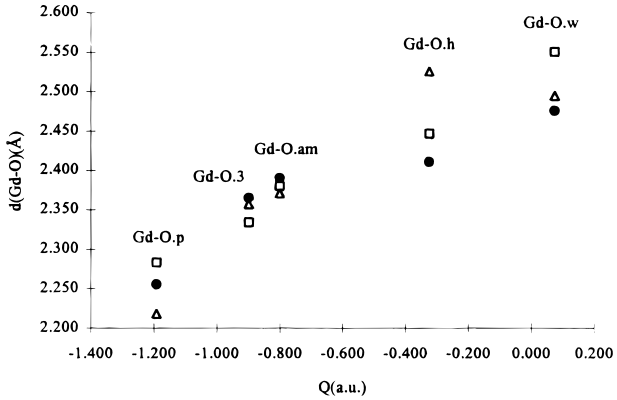

Figure 4. Experimetal (•), ab initio (□) and MM (Δ) Gd−O bond distance values (Å) versus oxygen average charges[31] (NPA, a.u.) for complexes with ligands **1**, **3**, **5b**, and **8a**.

8b only the **IA** is observed. Ab initio results show these isomers to be stationary points on the PES of $[Gd\cdot\mathbf{5b}\cdot OH_2]^{3+}$ and $[Gd\cdot\mathbf{8a}]^{1-}$, respectively.

The fact that the experimental and the optimized structures are similar is further confirmed by the rms values calculated on the Cartesian coordinates (Table 2). The coordination cages are described accurately at the ab initio level, as shown by the average value of the rms calculated for the three structures (0.081 Å). The increase in the rms values calculated on the whole structures is mainly due to the position of the pendent arms. Their being on the molecular surface makes these groups more susceptible to intermolecular interactions, which cause distortion with respect to what is found for isolated systems.

The oxygen position of the capping water molecule is close to the experimental one in the complex with **5b**, while in the complex with **3** the calculated bond distance between the ion and the water molecule is greater than the experimental value. This seems to be due to the presence of intramolecular hydrogen bonds between the alcoholic hydrogens and the water oxygen in the calculated structure.

An attempt was made to investigate the possibility of gadolinium coordinating one water molecule in the complex with the phosphinic ligand **8a** by optimizing the molecular structure of $[Gd\cdot\mathbf{8a}\cdot OH_2]^{1-}$ at the RHF/3-21G level. The results show that the Gd−water distance is 2.78 Å, highlighting the poor tendency of the water molecule to occupy the ninth coordination site.

In agreement with our previous results,[5] the calculated Gd−N bond distances are greater, on average, than the corresponding experimental values, while the Gd−O bonds are very close to the experimental ones (Table 1). As a consequence, the distance between the ion and the nitrogen plane is greater in the calculated structures than in the crystallographic ones. This is probably due to the lack of surrounding effects in the calculations; geometry optimizations at the RHF level on Ln−DOTA complexes performed in aqueous solutions[28] by means of the polarizable continuum model (PCM)[29] show that the Ln−L distances are closest to the experimental values and the ion is more deeply embedded in the coordination cage.

Experimental evidence revealed that the Gd−O bond distances found in the calculated structures can differ, depending on which donor oxygen atom is coordinated to the ion (Table 1, Figure 4). For example the shortest bond distances are shown by the phosphinic oxygens, these are followed by the carboxylic and amidic oxygens and then by the alcoholic and water oxygens, which have the greatest bond distance. The atomic charges on the oxygen atoms were considered as indexes of the degree of the interaction between the Gd ion and the different donor oxygen atoms and were derived from the natural population analysis (NPA)[30] at the RHF/3-21G level.[31] Thus, the increase in the electronic population on the oxygen is associated with the shortening of the Gd−O bond distance (Figure 4), as can be expected from a qualitative hardness scale of these donor oxygen atoms.

Force Field Parametrization and MM Calculations. *Force Field Parametrization.* The quality of the fitting of the empirical potential to the ab initio PES is highlighted by the results (Table 5) that present the same accuracy as those obtained[5] in the

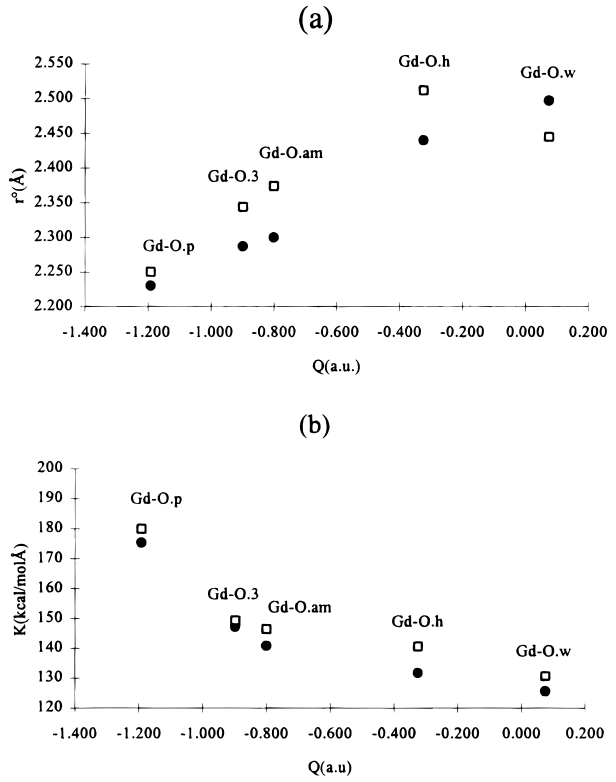

Figure 5. (a) $r°_{Gd-L}$ (Å); (b) K_{Gd-L} (kcal/ Å mol) versus oxygen average charges (NPA, a.u.). Data reported for Set 1 (•) and Set 1′(□).

parametrization of Gd interactions with DOTA (**1**). As previously observed, when the electrostatic contribution is included, the force field reacts with a shortening of the $r°$ values to counterbalance the electrostatic repulsion among the donor atoms (Table 4). Furthermore, the values of the derived parameters reflect the different Gd−O interactions: increasing the hardness of donor atoms, i.e., increasing the oxygen−ion interactions, causes a decrease in $r°$ and an increase in the stretching force constant values (Figure 5).

For the metal-independent parameters, coordination leads to structural variations in the bonds between atoms in position 2−3 with respect to the ion (C.3−C.3, C.2−C.3, and P.3−C.3) and in the angles between atoms in position 1−2−3 including a double bond (O.3−C.2═O.2, O.p−P.3═O.2, and O.am═C.2−N.am). Coordination to metal ions leads to similar variations for different classes of ligands,[8] such as, amine and carboxylic acid. The refined force field parameters for the "organic" part of the complex take these modifications into account efficiently.

Molecular Mechanics Calculations. With the aim of testing both the quality and the transferability of the developed parameters, MM geometry optmization of Gd complexes was performed by using the parameters Set 1 and Set 1′, respectively, obtained by including and omitting the electrostatic contribution. Calculations were performed on the compounds involved in the parametrization (training set) and on different complexes (test set).

According to the experimental data[10−14,16] the MM optimized structures present an inverted square antiprismatic coordination polyhedron for [Gd·**3**·OH_2]$^{3+}$ and [Gd·**8a**]$^{1-}$, a square antiprismatic geometry for [Gd·**4**·OH_2], [Gd·**5b**·OH_2]$^{3+}$, and [Gd·**6**·OH_2], and a distorted tricapped trigonal prism geometry for [Gd·**7a**·OH_2].

The rms values reported in Table 2 show that, generally speaking, MM reproduces the experimental structures with the same accuracy as ab initio methods, and calculations performed with both parameter sets provide similar results. Moreover, no significant differences are observed in the quality of the results obtained for the complexes included in the training and test sets, supporting the transferability of the developed parameters. As all the investigated complexes present not only amidic, alcoholic, and phosphinic oxygen donor atoms but also aminic and carboxylic donor groups, the good quality of the results confirms the transferability of the previously developed parameters for the Gd−PAC complexes.

As observed in the ab initio results, the greatest increment in rms values derives from the position of the pendent groups, the highest rms values being observed for the complex with the linear ligand **7a**. These results show the same quality as those previously obtained for PAC complexes.[5]

In all the MM optimized structures, the oxygen positions of the water molecules are close to the experimental. The water molecules assume different orientations depending on the adopted force fields: when the electrostatic contribution is omitted, the water hydrogen atoms point toward the external part of the complex; instead, when the electrostatic term is included, they are oriented toward the acetate oxygen atoms, as in ab initio structures, because of hydrogen bond interactions.

In general, the implemented sets of parameters reproduce the ab initio potential around the ion well, as highlighted by the quality of the fitting between the MM and ab initio structures (Table 2). The MM calculated Gd−N and Gd−O bond distances (Table 1) are respectively greater than and equal to the corresponding experimental values, as observed in ab initio results. Moreover, the MM calculated Gd−O distances present different values according to the different oxygen donor atoms coordinated to the ion (Figure 4). As observed in the experimental data and ab initio results, the phosphinic oxygens show the shortest bond distances, followed by carboxylic and amidic oxygens; alcoholic and water oxygens present the greatest bond distance values (Table 1).

Finally, to test the ability of the implemented force fields to reproduce the conformational energies of these systems, MM calculations were performed on the **A** and **IA** isomers of the complexes of Gd with the amidic ligands **5a**−**c** and the phosphinic ligand **8a** (Table 6). It is known experimentally from NMR measurements in solution on the europium complexes[15] that the **IA**/**A** ratio increases, increasing the steric hindrance around the ion, passing from 0.25 for [Eu·**5a**·OH_2]$^{3+}$, to 0.31 for [Eu·**5b**·OH_2]$^{3+}$ and 2.0 for [Eu·**5c**·OH_2]$^{3+}$. In the case of [Eu·**8a**]$^{1-}$ the steric demand around the phosphorus centers is such that only the **IA** isomer is evident in solution and the bound lanthanide ion is eight-coordinated. The MM results obtained by using the parameters derived with no electrostatic contribution (Set 1′) describe the experimental trend qualitatively; i.e., the stability of the **IA** species increases with the steric hindrance;

TABLE 6: Experimental[15] and MM Calculated (Set 1 and Set 1′) Relative Energies of the IA Isomer ($\Delta E = E_{IA} - E_A$, kcal mol^{-1}) for the Complexes of Gd with Ligands 5a−5c and 8a

	[Gd·**5a**·OH_2]$^{3+}$	[Gd·**5b**·OH_2]$^{3+}$	[Gd·**5c**·OH_2]$^{3+}$	[Gd·**8a**]$^{1-}$
exptl[a]	0.82	0.68	−0.41	[b]
MM Set 1	1.27	0.00	−2.76	−40.31
MM Set 1′	−3.82	−3.63	−4.43	−15.98

[a] From NMR measurements on the corresponding Europium complexes. [b] Only the **IA** isomer detected in solution.

however, it is only the inclusion of the electrostatic contribution in the force fields (Set 1) that leads to the appropriate relative stability between the two isomers.

In conclusion, the two sets of MM parameters describe the geometrical features of the investigated Gd complexes with the same accuracy as ab initio calculations, but the inclusion of the electrostatic contribution in the force fields is necessary for a reliable description of the conformational behavior of these systems, as previously observed[5] for the case of Gd−PAC complexes. Moreover, as the complex−solvent interactions play a crucial role in the use of the complexes as MRI contrast agents, the electrostatic contribution must be included in the empirical potential for an adequate modeling of this class of compounds.

IV. Conclusions

The successful extension of the force fields to complexes of gadolinium with ligands presenting amidic, alcoholic, and phosphinic oxygen donor atoms permitted us to validate the developed parametrization procedure. Moreover, the quality of the MM results obtained allowed us to check the transferability of the derived parameters to a larger set of compounds, including complexes presenting different types of oxygen donor atoms in the same coordination cage. Thus, we found the adopted procedure to be reliable for the parametrization of metal−ligand interactions providing accurate results at reasonable computational cost. Moreover, the procedure based on ab initio calculations can be used confidently, even if experimental data are not available.

Two general aspects of the procedure should be highlighted. First, unlike force fields parameters derived from experimental data in condensed phase, the parameters obtained by this procedure refer to the isolated molecule model and thus do not take the surrounding effects into account. On the other hand, it is this model itself that seems the most suitable for parameter development: in fact, nowadays the surrounding effects can be included explicitly by means of several computational approaches, both at the quantum mechanical and the MM level.

Second, derived parameters are implicitly characterized by the theory level and basis sets used in the ab initio calculations; thus, the limits and characteristics of the theory framework are always well defined. In our case, for instance, it is well-known that HF level calculations, not including dynamic electron correlation effects, provide force constants roughly 10−15% too large and do not take dispersion interactions into account. Increasing computer power and software development will make the investigation of such molecular systems possible at higher and higher quantum mechanical levels, allowing force fields parameter refinement.

Finally, we can conclude that the extension of force fields to ligands linked to the gadolinium ion by amidic, alcoholic, and phosphinic oxygen donor atoms widens the typology of complexes that can be investigated, increasing the ability of computational simulation in supporting the rational design of new contrast agents with predetermined structures and properties.

Acknowledgment. Financial support from the Italian National Research Council (CNR, Target Project on Biotechnology, Grant 97.01081.PF49) and the Italian Ministry of Scientific and Technological Research (Grant MURST 60%) is gratefully acknowledged.

References and Notes

(1) (a) Caravan, P.; Ellison, J. J.; McMurry, T. J.; Lauffer, R. B. *Chem. Rev.* **1999**, *99*, 2293. (b) Lauffer, R. B. *Magn. Res. Quarterly* **1990,** *6*, 65. (c) Tweedle, M. F. In *Lanthanide Probes in Life, Chemical and Earth Sciences*; Bünzli, J. C. G., Choppin, G. R., Eds.; Elsevier: Amsterdam, 1989. (d) Lauffer, R. B. *Chem. Rev.* **1987**, *87*, 901.

(2) ID numbering and abbreviated names for the ligands: (**1**) DOTA = 1,4,7,10-tetraazacyclododecane 1,4,7,10-tetraacetate; (**2**) DTPA = 1,4,7-triazaheptane 1,1,4,7,7-pentaacetate; (**3**) THP = 1,4,7,10-tetrakis (2-hydroxypropyl)-1,4,7,10-tetraazacyclododecane; (**4**) HP-DO3A = 10-(2-hydroxypropyl)-1,4,7,10-tetraazacyclododecane-1,4,7-tetraacetate; (**5a**) DOTAM = 1,4,7,10-tetrakis[carbamoylmethyl]-1,4,7,10-tetraazacyclododecane; (**5b**) TMA = 1,4,7,10-tetrakis[(*N*-methylcarbamoyl)methyl]-1,4,7,-10-tetraazacyclododecane; (**5c**) DOTTA = 1,4,7,10-tetrakis [(N,N-dimethylcarbamoyl)methyl]-1,4,7,10-tetraazacyclododecane; (**6**) DOTA-MA = 10-[(*N*-methylcarbamoyl)methyl]-1,4,7,10-tetraazacyclododecane-1,4,7- tetraacetate; (**7a**) DTPA-BMA = 1,7-bis[(*N*-methylcarbamoyl)methyl]-1,4,7-triazaheptane-1,4,7- pentaacetate; (**7b**) DTPA-BEA = 1,7-bis[(*N*-ethylcarbamoyl)methyl]-1,4,7-triazaheptane-1,4,7- pentaacetate; (**8a**) DOTMP = 1,4,7,10-tetraazacyclododecane-1,4,7,10-tetrakis(methylenemethylphosphinate); (**8b**) DOTBzP = 1,4,7,10-tetraazacyclododecane-1,4,7,10-tetrakis-(methylenebenzylphosphinate).

(3) Christiansen, P. A.; Ermler, W. C.; Pitzer, K. S. *Annu. Rev. Phys. Chem.* **1985**, *36*, 407.

(4) Krauss, M.; Stevens, W. J. *Annu. Rev. Phys. Chem.* **1984**, *35*, 357.

(5) Cosentino, U.; Moro, G.; Pitea, D.; Villa, A.; Fantucci, P. C.; Maiocchi, A.; Uggeri, F. *J. Phys. Chem. A* **1998**, *102*, 4606.

(6) (a) Hay, B. P. *Inorg. Chem.* **1991**, *30*, 2876. (b) Cundari, T. R.; Moody, E. W.; Sommerer, S. O. *Inorg. Chem.* **1995**, *34*, 5989. (c) Beech, J.; Drew, M. G. B.; Leeson, P. B. *Struct. Chem.* **1996**, *7*, 153. (d) Fossheim, R.; Dahl, S. G. *Acta Chem. Scand.* **1990**, *44*, 698. (e) Comba, P.; Gloe, K.; Inoue, K.; Krüger, T.; Stephan, H.; Yoshizuka, K. *Inorg. Chem.* **1998**, *37*, 3310.

(7) Comba, P.; Hambley, T. W. *Molecular Modelling of Inorganic Compounds*; VCH Publishers Inc.: New York, 1995.

(8) Bol, J. E.; Buning, C.; Comba, P.; Reedijk, J.; Ströhle, M. *J. Comput. Chem.* **1998**, *19*, 512.

(9) Maple, J. R.; Hwang, M. J.; Stockfish, T. P.; Dinur, U.; Waldman, M.; Ewig, C. S.; Hagler, A. T. *J. Comput. Chem.* **1994**, *15*, 162.

(10) Chin, K. O. A.; Morrow, J. R.; Lake, C. H.; Churchill, M. R. *Inorg. Chem.* **1994**, *33*, 656.

(11) Kumar, K.; Chang, C. A.; Francesconi, L: C.; Dischino, D. D.; Malley, M. F.; Gougoutas, J. Z.; Tweedle, M. F. *Inorg. Chem.* **1994**, *33*, 3567.

(12) Alderighi, L.; Bianchi, A.; Calabi, L.; Dapporto, P.; Giorgi, C.; Losi, P.; Paleari, L.; Paoli, P.; Rossi, P.; Valtancoli, B.; Virtuani, M. *Eur. J. Inorg. Chem.* **1998**, 1581.

(13) Aime, S.; Anelli, P. L.; Botta, M.; Fedeli, F.; Grandi, M.; Paoli, P.; Uggeri, F. *Inorg. Chem.* **1992**, *31*, 2422.

(14) Konings, M. S.; Dow, W. C.; Love, D. B.; Raymond, K. N.; Quay, S. C.; Rocklage, S. M. *Inorg. Chem.* **1990,** *29*, 1488.

(15) Aime, S.; Barge, A.; Bruce, J. I.; Botta, M.; Howard, J. A. K.; Moloney, J. M.; Parker, D.; de Sousa, A. S.; Woods, M. *J. Am. Chem. Soc.* **1999**, *121*, 5762.

(16) Aime, S.; Batsanov, A. S.; Botta, M.; Howard, J. A. K.; Parker, D.; Senanayake, K.; Williams, G. *Inorg. Chem.* **1994**, *33*, 4696.

(17) Tóth., E.; Platzek, K. J.; Radüchel, B.; Brücher, E. *Inorg. Chim. Acta* **1996**, *248*, 193.

(18) Gaussian94, Revision B.3, Frisch, M. J.; Trucks, G. W.; Schlegel, H. B.; Gill, P. M. W.; Johnson, B. G.; Robb, M. A.; Cheeseman, J. R.; Keith, T.; Petersson, G. A.; Montgomery, J. A.; Raghavachari, K.; Al-Laham, M. A.; Zakrzewski, V. G.; Ortiz, J. V.; Foresman, J. B.; Peng, C. Y.; Ayala, P. Y.; Chen, W.; Wong, M. W.; Andres, J. L.; Replogle, E. S.; Gomperts, R.; Martin, R. L.; Fox, D. J.; Binkley, J. S.; Defrees, D. J.; Baker, J.; Stewart, J. P.; Head-Gordon, M.; Gonzalez, C.; Pople, J. A. Gaussian, Inc.: Pittsburgh, PA, 1995.

(19) Dolg, M.; Stoll, H.; Savin, A.; Preuss, H. *Theor. Chim. Acta* **1989**, *75*, 173.

(20) Cosentino, U.; Moro, G.; Pitea, D.; Calabi, L.; Maiocchi, A. *J. Mol. Struct. THEOCHEM* **1997**, *392*, 75.

(21) Tripos Associates, 1699 S. Hanley Road, Suite 303, St. Louis, MO, 63144, SYBYL 6.3 1996.

(22) Clark, M.; Cramer III, R. D.; Van Opdenbosch, N. *J. Comput. Chem.* **1989**, *10*, 982.

(23) (a) Hambley, T. W. *Inorg. Chem.* **1991**, *30*, 937. (b) Hay, B. P. *Coord. Chem. Rev.* **1993**, *126*, 177.

(24) Potential derived charges were calculated on the RHF/3-21G optimized geometries for Gd complexes with ligands **3**, **5b**, and **8a** and on MM-Set 1′ optimized geometries for complexes with ligands **4**, **5a**, **5c**, **6**, and **7a**. Then, as the charges of the atoms represented by the same MM atom-type were similar, their average value was used in the MM calculations in each compound.

(25) Besler, B. H.; Merz, K. M.; Kollman, P. A. *J. Comput. Chem.* **1990**, *11*, 431.

(26) List of the TRIPOS force fields atom types used in the definition of the investigated Gd complexes: Gd (gadolinium); C.3 (sp^3 carbon); C.2

(sp^2 carbon); N.4 (tetracoordinated sp3 nitrogen); P.3 (phosphorus) O.3 (sp^3 carboxylic oxygen); O.2 (sp^2 carboxylic oxygen); O.am (sp^2 amidic oxygen); O.h (sp^3 alcoholic oxygen); O.p (sp^3 phosphinic oxygen); O.w (sp^3 water oxygen); H (hydrogen); H.w (water hydrogen). In all cases, TRIPOS default atomic parameter values are used. The O.w and H.w atom types have been included only with the purpose of distinguishing the water O and H from the ligand O and H: the atomic parameters for O.w and H.w have been set equal to those of O.3 and H, respectively.

(27) Depending on whether electrostatic contribution is turned on (off): $w_g = 1 \times 10^{3-}$ ($1 \times 10^{3-}$) for $[Gd\cdot\mathbf{3}\cdot OH_2]^{3+}$; $w_g = 1 \times 10^{3-}$ ($5 \times 10^{4-}$) for $[Gd\cdot\mathbf{5b}\cdot OH_2]^{3+}$; $w_g = 2 \times 10^{4-}$ ($2 \times 10^{4-}$) for $[Gd\cdot\mathbf{8a}]^{1-}$. In any case, $w_E = 1$.

(28) Cosentino, U.; Pitea, D.; Villa, A.; Moro, G.; Barone V. Manuscript in preparation.

(29) Tomasi, J.; Persico, M. *Chem. Rev.* **1994,** *94*, 2027.

(30) Reed, A. E.; Weinstock, R. B.; Weinhold, F. *J. Chem. Phys.* **1985**, *83*, 735.

(31) In the case of alcoholic and water oxygens the considered atomic charges were obtained by adding the hydrogen charges to the oxygen.